Classical versus Nonclassical Covalent Bonding between the Metal Hydride Radicals MH and M′H_j (MH = HBe, HMg, HCa; M′H_j = Li, BeH, BH_2, Na, MgH, AlH_2, K, CaH, GaH_2)

Eric Magnusson and Simon Petrie*,†

School of Chemistry, University College, University of New South Wales, ADFA, Canberra, ACT 2600 Australia

Received: April 29, 2003; In Final Form: June 13, 2003

We report structures, bond strengths, and relative energies for all apparent minima on the B3LYP/6-311+G** potential energy surfaces of the main group compounds [MH_{j+1}M′] formed between the first three metal hydride radicals of group 2 (MH) and the first three metal hydride radicals of groups 1, 2, and 13 (M′H_j). Relative energies and bond strengths at the G2(MP2)thaw level of theory, using the B3-LYP/6-311+G** optimized geometries, have also been obtained: the G2(MP2)thaw values conform closely to the B3-LYP results. Significant structural trends identified include the characterization of at least one competing "nonclassical" isomer for each of the 24 classical HM−M′H_j structural formulas, an increasing preference for nonclassical rather than classical bonding as M is switched from Be to Mg to Ca, and an increased tendency toward stability of unorthodox structures as M′ progresses from group 1 to 2 to 13. An exploration of the factors underpinning bond formation between M and M′, focusing particularly on the three [CaHNa] isomers we have located, has been undertaken using the atoms-in-molecules (AIM) computational method. Although our AIM calculations confirm that the metal−metal bonds are largely covalent in character, some aspects of the bonding remain mysterious. Prospects for experimental investigation of polymorphism, via matrix isolation or other techniques, appear to be particularly promising for [MgH_2Ca], for which four distinct structural isomers are separated by only approximately 30 kJ mol^{-1}.

Introduction

Electropositive atoms are generous with their valence electrons, but they do not share them gracefully. The bonds between main-group metal atoms are among the weakest examples seen across the spectrum of covalently bonded structures, and isolation of species containing a nominal intermetallic bond is beset by much difficulty. As a consequence, very little is known of the structure of main-group intermetallic compounds.

We have conducted a systematic survey of the structural and energetic properties of the set of main-group binuclear hydrides $H_iM-M'H_j$ (H_iM, $M'H_j \in$ {H, Li, HBe, H_2B, H_3C, ..., H_2As, HSe, Br}) in which the focus is on the factors influencing the strength of the central, nominally covalent M−M′ bond. The formulas are all capable of being represented by the classical structure of a direct single bond between the heavy atoms both of which are valence-saturated with hydrogen atoms. Pairings between the 22 different monovalent radicals {H, Li, HBe, ..., Br} yield 253 distinct structural formulas, and within this range of compounds, the subset of intermetallic molecules is notable both for the sparseness of theoretical and experimental data and for the degree of polymorphism evident in their structures. For example, in the sole study reported to date on the [AlH_4Ga] potential energy surface, Leszczynski and Lammertsma[1] have identified a remarkable total of eight distinct isomers for this species[2] encompassing the classical covalently bonded species H_2AlGaH_2 and a variety of bridged and saltlike structures. Although the intermetallic compounds surveyed in the present work lack the degree of structural versatility seen for [AlH_4-Ga], they remain noteworthy for the insight they permit concerning the struggle between classical covalent and nonclassical bonding motifs in electron-deficient compounds.

Of the species covered in the present work, experimental isolation has been reported only for the homonuclear dimers [MH_2M] (M = Be,[3] Mg,[4] and Ca[5]). In all three instances, these species were generated by reaction with H_2 of metal atoms, followed by isolation in a rare-gas matrix. The range of theoretical studies on these species is somewhat greater—previous studies have featured [BeHLi],[6−12] [BeH_2Be],[3,10,12−17] [BeH_3B],[10,12,18,19] [BeH_3Al],[20] [MgHLi],[9] [MgH_3B],[19] [CaH_3B],[19] [MgH_2Mg],[4,14,21] [MgH_3Al],[22] and [CaH_3Al].[23] Some earlier surveys of energetic trends in covalent bond strength have also featured several examples of these species drawn from the first row[24,25] or from the first two rows[26] of the periodic table: however, those surveys appear not to have investigated any bridged or nonclassical structures for these species. The focus in the previous theoretical studies has largely been on the lightest members of the [MH_{j+1}M′] set, and the coverage of third-row-containing species is particularly sparse. In the present study, therefore, we have aimed to fill a number of gaps by presenting a systematic comparison of intermetallic [MH_{j+1}M′] compounds (M = Be, Mg, Ca; M′H_j = Li, BeH, BH_2, Na, MgH, AlH_2, K, CaH, GaH_2), involving high-level ab initio and density functional theory calculations, and to explore the trends in bond strength and structural form within these compounds. We have also employed the atoms-in−molecules (AIM) approach[27] for a more in-depth analysis of the intermetallic bonding seen in these species.

Theoretical Methods

Optimized geometries, total energies, and zero-point vibrational energies of the stationary points on the [MH_{j+1}M′]

* To whom correspondence should be addressed.
† Present address: Department of Chemistry, the Faculties, Australian National University, Canberra ACT 0200 Australia. E-mail: simon.petrie@anu.edu.au.

10.1021/jp0351526 CCC: $25.00
Published on Web 08/13/2003

TABLE 1: Frozen Core Assignments Used for Combinations of Metallic Elements[a]

	M′								
M	Li	Be	B	Na	Mg	Al	K	Ca	Ga
Be	1s/1s	1s/1s	1s/1s	1s/2p	1s/2p	1s/2p	1s/2p	1s/2p	1s/3p
Mg	2p/1s	2p/1s	2p/1s	1s/1s	1s/1s	2p/2p	1s/2p	1s/2p	1s/3p
Ca	2p/1s	2p/1s	2p/1s	2p/1s	2p/1s	2p/2p	2p/2p	2p/2p	2p/3p

[a] Orbitals shown denote the outermost extent of the frozen core on M and M′, respectively, in MP2/6-311+G(3df,2p) and QCISD(T)/6-311G** calculations on the intermetallic hydrides.

potential energy surfaces were obtained at the B3-LYP/6-311+G** level of theory. Further single-point total energy calculations on the stationary point geometries were undertaken at the MP2/6-311+G(3df,2p) and QCISD(T)/6-311G** levels of theory, to provide G2(MP2) relative energies. The G2(MP2) method was selected as the most appropriate "model chemistry" method for these species because of its economy, reliability, and applicability to compounds comprised of atoms from the first three rows of the periodic table.[28−31] However, implementation of the standard frozen-core approximation in G2(MP2), G2, and related methods[32−36] has been indentified as inappropriate for some calculations on compounds containing main-group metals; consequently, to improve the reliability of the G2(MP2) values, nonstandard or "thawed" correlation spaces[32−34] were assigned in several instances as identified in Table 1.

The structural preferences of various metal−metal combinations were studied by performing B3LYP calculations at the minimal basis set level and using scale factor variation to alter the effective nuclear charge parameter for the basis sets of one element at a time. Use of the STO-3G minimal basis set ensured that variation in Z_{eff} did not engender compensating changes in other parts of the wave function.

All calculations were performed using the GAUSSIAN98 suite of programs.[37]

Results and Discussion

In the discussion throughout this paper, we distinguish between the term "orthodox", by which we denote a compound that for each atom has a cumulative bond order formally equal to that atom's valency, and the term "classical", which describes a compound formally possessing only two-center, two-electron bonds. Note that some of the unorthodox stationary points investigated here (for the $[MH_3M']$ compounds only, where M′ is a group 13 element) are nevertheless classical according to these definitions.

Structural and Energetic Tendencies: An Overview. Optimized geometries (obtained at the B3-LYP/6-311+G** level), total energies, and bond dissociation energies (at B3-LYP/6-311+G** and G2(MP2)thaw) for the various stationary points are shown in Tables 2−7. Perusal of these tables reveals several notable features, which we summarize below:

(i) For all structural formulas considered here, there always exists at least one unorthodox isomer in competition with the orthodox $HM-M'H_j$ structure.

(ii) When the molecule contains a first-row group 2 metal atom M, orthodox structures are preferred: only $[BeH_3Al]$ and $[BeH_3Ga]$ of the eight beryllium compounds have unorthodox global minima. Conversely, when a third-row (group 2) M is featured, only three compounds of the eight possess *orthodox* global minima. The formulas are $[CaH_2Be]$, [CaHNa], and [CaHK] and in all three the preference for the orthodox form is comparatively slight. There is thus a clear tendency, with progression down the group, toward increasing stability of structures having an unorthodox connectivity of atoms.

TABLE 2: Stationary Points on the [MHM′] Potential Energy Surfaces, Obtained at the B3-LYP/6-311+G Level of Theory**

formula	structure	M−M′ [a]	H−M[a]	H−M′ [a]	∠HMM′ [b]
HBeLi ($C_{\infty v}$)	**I**	2.400	1.354		180
BeHLi ($C_{\infty v}$)	**I***n*(1)		1.576	1.697	
Be(H)Li (C_s)	**I***n*(2)	2.196	1.523	1.712	51.0
HMgLi ($C_{\infty v}$)	**I**	2.765	1.748		180
MgHLi ($C_{\infty v}$)	**I***n*(1)		2.308	1.623	
Mg(H)Li (C_s)	**I***n*(2)	2.746	2.282	1.620	36.1
HCaLi ($C_{\infty v}$)	**I**	3.237	2.029		180
CaHLi ($C_{\infty v}$)	**I***n*(1)		2.292	1.646	
Ca(H)Li (C_s)	**I***n*(2)	2.946	2.234	1.653	33.8
HBeNa ($C_{\infty v}$)	**I**	2.663	1.354		180
BeHNa ($C_{\infty v}$)	**I***n*(1)		1.504	2.034	
HMgNa ($C_{\infty v}$)	**I**	2.989	1.748		180
MgHNa ($C_{\infty v}$)	**I***n*(1)		2.059	1.962	
HCaNa ($C_{\infty v}$)	**I**	3.428	2.022		180
CaHNa ($C_{\infty v}$)	**I***n*(1)		2.236	1.981	
Ca(H)Na (C_s)	**I***n*(2)	3.164	2.164	2.069	40.6
HBeK ($C_{\infty v}$)	**I**	3.124	1.362		180
BeHK ($C_{\infty v}$)	**I***n*(1)		1.488	2.399	
HMgK ($C_{\infty v}$)	**I**	3.465	1.764		180
MgHK ($C_{\infty v}$)	**I***n*(1)		2.046	2.325	
Mg(H)K (C_s)	**I***n*(2)	3.363	2.090	2.323	43.0
HCaK ($C_{\infty v}$)	**I**	3.911	2.028		180
CaHK ($C_{\infty v}$)	**I***n*(1)		2.217	2.344	
Ca(H)K (C_s)	**I***n*(2)	3.582	2.147	2.404	40.7

[a] Optimized bond length in ångstroms. [b] Optimized bond angle in degrees.

(iii) When the "heteroatom" M′ is group 1, only one of the nine formulas, namely [CaHLi], has an unorthodox global minimum. When M′ is group 2, two formulas out of 6, $[MgH_2Ca]$ and $[CaH_2Ca]$, have unorthodox global minima; when M′ is group 13, the corresponding value is 8 of 9 compounds. Therefore, progression of M′ from group 1 through 2 to 13 clearly leads to an increased preference for unorthodox structures.

Three broad categories of unorthodox structures can be discerned. First, the structure may feature one or more bridging hydrogens that augment the M−M′ bond. Second, the direct M−M′ bond may be supplanted by two-electron, three-center M(H)M′ bonds. (These first two structural motifs are both therefore nonclassical by virtue of possessing three-center bonds.) Third, a direct M−M′ bond may exist in a structure in which all the hydrogens are formally bonded to M′. Schematic examples of such bonding patterns, shown in Figure 1, are respectively **I***n*(2), **II***n*(3), and **XIII***ht*, where the Roman numeral signifies the group number of the "heteroatom" M′, the *n* notation indicates a nonclassical structure, and *ht* denotes a "hydride transfer" structure that is unorthodox but nevertheless classical because it lacks bridging hydrogens. The labels shown in Figure 1 are used throughout this discussion, and in Tables 2−7, so as to distinguish between the various isomers. Note, however, that description of a structure as, for example, **II***n*(2) does not necessarily indicate the presence, nor absence, of a direct M−M′ bond. A more rigorous assessment of bonding requires an analysis such as has been undertaken, for some of these compounds, using the AIM (atoms-in−molecules) approach, which is detailed in a subsequent subsection.

In the following subsections, we discuss in greater detail the specific features of the [MHM′] (M′ from group 1), $[MH_2M']$ (M′ from group 2), and $[MH_3M']$ (M′ from group 13) potential energy surfaces.

[MHM′] Structures. These group-1-containing species, detailed in Tables 2 and 5, all feature two distinct linear structures M′MH (**I**) and M′HM (**I***n*(1)), both of which are

TABLE 3: Stationary Points on the [MH_2M'] Potential Energy Surfaces, Obtained at the B3-LYP/6-311+G Level of Theory**

formula	structure	M−M′ [a]	H−M[a]	∠HMM′ [b]	M′−H[a]	∠MM′H[b]	∠HMM′H[c]
HBeBeH ($D_{\infty h}$)	**II**	2.082	1.336	180	1.336	180	
BeH_2Be (D_{2h})	**II***n*(3)	2.071	1.513	46.8	1.513	46.8	180
HBeMgH ($C_{\infty v}$)	**II**	2.484	1.340	180	1.719	180	
BeHMgH ($C_{\infty v}$)	**II***n*(2)	5.148	3.441	0	1.706	180	
HBeCaH ($C_{\infty v}$)	**II**	2.944	1.350	180	2.036	180	
Be(H)CaH (C_s)	**II***n*(2)	2.630	1.498	57.3	2.010	173.3	0
HMgMgH ($D_{\infty h}$)	**II**	2.861	1.725	180	1.725	180	
MgHMgH ($C_{\infty v}$)	**II***n*(1)	5.772	4.066	0	1.706	180	
$Mg(H)_2Mg$ (D_{2h})	**II***n*(3)	2.857	1.924	42.1	1.924	42.1	180
HMgCaH (C_s)	**II**	3.328	1.740	179.4	2.022	174.5	180
HMgHCa ($C_{\infty v}$)	**II***n*(1)	4.736	1.701	180	3.012	0	
Mg(H)CaH (C_s)	**II***n*(2)	3.182	2.227	40.5	2.019	177.7	180
$Mg(H)_2Ca$ (C_{2v})	**II***n*(3)	3.175	1.951	41.6	2.149	37.0	180
HCaCaH ($D_{\infty h}$)	**II**	3.797	2.016	180	2.016	180	
Ca(H)CaH (C_s)	**II***n*(1)	3.420	2.201	36.7	2.017	172.2	0
$Ca(H)_2Ca$ (D_{2h})	**II***n*(3)	3.501	2.179	36.5	2.179	36.5	180

[a] Optimized bond length in ångstroms. [b] Optimized bond angle in degrees. [c] Optimized dihedral angle in degrees.

TABLE 4: Stationary Points on the [MH_3M'] Potential Energy Surfaces, Obtained at the B3-LYP/6-311+G Level of Theory**

formula	structure	M−M′ [a]	H−M[a]	∠HMM′ [b]	M′−H[a]	∠MM′H[b]	∠HMM′H[c]
$HBeBH_2$ (C_{2v})	**XIII**	1.868	1.331	180	1.198	123.4	
$HBe(H)_2B$ (C_{2v})	**XIII***n*(1)	2.045	1.324	180	1.328	48.5	
$BeBH_3$ (C_{3v})	**XIII***n*(2)	1.956			1.200	95.0	
$HBeAlH_2$ (C_{2v})	**XIII**	2.338	1.334	180	1.596	122.7	
$HBe(H)_2Al$ (C_{2v})	**XIII***n*(1)	2.485	1.335	180	1.864	35.5	
$BeAlH_3$ (C_{3v})	**XIII***n*(2)	2.653			1.592	93.9	
$HBeGaH_2$ (C_{2v})	**XIII**	2.266	1.331	180	1.582	123.8	
$HBe(H)_2Ga$ (C_{2v})	**XIII***n*(1)	2.527	1.338	180	1.929	35.0	
$BeGaH_3$ (C_{3v})	**XIII***n*(2)	2.555			1.572	93.8	
$HMgBH_2$ (C_{2v})	**XIII**	2.288	1.714	180	1.200	123.4	
$HMg(H)_2B$ (C_{2v})	**XIII***n*(1)	2.540	1.707	180	1.268	54.6	
$MgBH_3$ (C_{3v})	**XIII***n*(2)	2.438			1.196	93.1	
$HMgAlH_2$ (C_{2v})	**XIII**	2.738	1.714	180	1.601	123.5	
$HMg(H)_2Al$ (C_{2v})	**XIII***n*(1)	2.899	1.703	180	1.831	39.5	
$MgAlH_3$ (C_{3v})	**XIII***n*(2)	3.072			1.590	93.4	
$HMgGaH_2$ (C_{2v})	**XIII**	2.659	1.712	180	1.589	124.4	
$HMg(H)_2Ga$ (C_{2v})	**XIII***n*(1)	2.916	1.705	180	1.886	39.4	
$MgGaH_3$ (C_{3v})	**XIII***n*(2)	2.960			1.571	93.1	
$HCaBH_2$ (C_s)	**XIII**	2.664	2.027	139.2	1.207	125.0	±89.0
$HCaBH_2$ (C_s)	**XIII***r*	2.670	2.031	141.2	1.207 (1.206)	122.1 (127.8)	0 (180)
$HCa(H)_2B$ (C_s)	**XIII***n*(1)	2.259	1.996	177.2	1.248	80.1	±128.6
$CaBH_3$ (C_{3v})	**XIII***n*(2)	2.698			1.198	92.9	
$HCaAlH_2$ (C_{2v})	**XIII**	3.184	2.023	180	1.613	125.5	
$HCa(H)_2Al$ (C_{2v})	**XIII***n*(1)	3.252	2.029	180	1.829	40.0	
$CaAlH_3$ (C_{3v})	**XIII***n*(2)	3.390			1.592	94.2	
$HCaGaH_2$ (C_{2v})	**XIII**	3.080	2.023	180	1.605	126.5	
$HCa(H)_2Ga$ (C_{2v})	**XIII***n*(1)	3.263	2.031	180	1.879	40.2	
$CaGaH_3$ (C_{3v})	**XIII***n*(2)	3.235			1.573	93.9	

[a] Optimized bond length in ångstroms. [b] Optimized bond angle in degrees. [c] Optimized dihedral angle in degrees.

consistently found to be true minima (i.e., lacking any imaginary vibrational frequencies) according to our B3-LYP/6-311+G** calculations. In all instances, **I** is seen to be lower-energy than **I***n*(1), with the energy difference between isomers being ∼90−120 kJ mol^{-1} when M is Be, but with a markedly smaller relative energy gap (<50 kJ mol^{-1}) when M is Mg or Ca; in the case of [CaHLi], the relative energies of **I** and **I***n*(1) are too close to be certain that **I** is indeed the lower-energy of the two linear isomers. For M′ = Li (but not always for M′ = Na or K), it is also possible to isolate "bridged" structures **I***n*(2), which when they exist, are generally somewhat lower in energy than the linear nonclassical structures **I***n*(1); in the case of [CaHLi], **I***n*(2) is the apparent global minimum.

A comparison with the previous study by Tikilyainen et al.[9] is pertinent, because these authors have also considered the relative energies of isomers **I**, **I***n*(1), and **I***n*(2) in calculations using HF, MP2, and MP3, for the species [BeHLi] and [MgHLi]. Though their results for the [BeHLi] surface are in good accord with ours, they predict a much lower degree of stability (i.e., E_{rel} = 90 kJ mol^{-1})[9] than we find for **I***n*(2) on the [MgHLi] surface.

The H−M′ distances in the nonclassical isomers for all of these compounds suggests the presence of formal H-alkali metal bonds in these structures, which to some extent can be viewed as molecular combinations of the alkaline earth atoms M and the alkali hydrides M′H. The bond strengths for these combinations, calculated on the basis of the G2(MP2)thaw total energies for the appropriate species, are detailed in Table 8. It is apparent that these M/M′H interactions are all rather weak when assessed against the "normal" range expected for a full covalent single bond, of 200−400 kJ mol^{-1}. Nonetheless, both the M−H bond lengths in Table 2 and the bond strengths in Table 8 suggest that these are not merely van der Waals-type interactions, and in some cases it is reasonable to expect that the calculated

TABLE 5: Calculated Total, Bond, and Relative Energies of Isomers on the [MHM′] PES

		B3-LYP/6-311+G**				G2(MP2)thaw			
formula	structure	E_e,[a] hartrees	ZPE,[b] mhartrees	D_0(M−M′),[c] kJ mol^{-1}	E_{rel},[d] kJ mol^{-1}	E_0,[e] hartrees	$\Delta H_f°$,[f] kJ mol^{-1}	D_0(M−M′),[c] kJ mol^{-1}	E_{rel},[d] kJ mol^{-1}
HBeLi	**I**	−22.82056	7.608	160.2	0	−22.69690	323.2	184.8	0
BeHLi	**I***n*(1)	−22.77104	5.139	36.7	123.5	−22.65083	444.1	63.8	121.0
Be(H)Li	**I***n*(2)	−22.78420	6.053	68.8	91.4	−22.66604	404.2	103.7	81.1
HMgLi	**I**	−208.19051	5.390	129.6	0	−207.68222	247.8	154.6	0
MgHLi	**I***n*(1)	−208.18423	4.104	116.4	13.1	−207.67376	270.0	132.4	22.2
Mg(H)Li	**I***n*(2)	−208.18717	4.505	123.1	6.4	−207.67726	260.8	141.5	13.1
HCaLi	**I**	−685.67626	4.054	95.1	0	−685.08684	288.4	160.9	0
CaHLi	**I***n*(1)	−685.67625	4.899	92.9	2.2	−685.08649	289.3	160.0	0.9
Ca(H)Li	**I***n*(2)	−685.68334	5.079	111.0	−15.9	−685.09412	269.3	180.0	−19.1
HBeNa	**I**	−177.60385	7.082	129.5	0	−177.09829	305.9	151.8	0
BeHNa	**I***n*(1)	−177.55736	5.521	11.5	118.0	−177.05378	422.8	34.9	116.9
HMgNa	**I**	−362.97864	4.980	111.3	0	−362.35344	220.7	137.1	0
MgHNa	**I***n*(1)	−362.96448	4.236	76.0	35.2	−362.33713	263.5	94.2	42.9
HCaNa	**I**	−840.46794	3.859	85.6	0	−839.61809	287.3	111.7	0
CaHNa	**I***n*(1)	−840.45748	4.571	56.2	29.3	−839.60664	317.4	81.7	30.0
Ca(H)Na	**I***n*(2)	−840.45607	4.049	53.9	31.7	−839.61088	306.2	92.8	18.9
HBeK	**I**	−615.23591	6.634	107.5	0	−614.63672	307.4	132.7	0
BeHK	**I***n*(1)	−615.19878	5.110	14.0	93.5	−614.59972	404.6	35.5	97.2
HMgK	**I**	−800.61288	4.613	94.8	0	−799.75553	217.7	122.4	0
MgHK	**I***n*(1)	−800.60338	3.739	72.1	22.6	−799.74484	245.8	94.3	28.1
Mg(H)K	**I***n*(2)	−800.60102	3.666	66.1	28.7	−799.74845	236.3	103.8	20.6
HCaK	**I**	−1278.10326	3.820	71.0	0	−1277.01875	288.1	93.3	0
CaHK	**I***n*(1)	−1278.09795	4.136	56.3	14.8	−1277.01420	300.1	81.3	12.0
Ca(H)K	**I***n*(2)	−1278.09944	3.915	60.7	10.3	−1277.01839	289.0	92.4	0.9

[a] Total energy, excluding ZPE. [b] Zero-point vibrational energy. [c] Calculated bond dissociation energy, at the indicated level of theory (and at 0 K), for dissociation to M′ + MH. [d] Total energy, including ZPE, expressed relative to isomer **I**. [e] Total energy, including ZPE, at 0 K, according to G2(MP2)thaw calculations employing the B3-LYP/6-311+G** optimized geometry. [f] Calculated enthalpy of formation at 0 K.

TABLE 6: Calculated Total, Bond, and Relative Energies of Isomers on the [MH_2M'] Pes

		B3-LYP/6-311+G**				G2(MP2)thaw			
formula	structure	E_e,[a] hartrees	ZPE,[b] mhartrees	D_0(M−M′),[c] kJ mol^{-1}	E_{rel},[d] kJ mol^{-1}	E_0,[e] hartrees	$\Delta H_f°$,[f] kJ mol^{-1}	D_0(M−M′),[c] kJ mol^{-1}	E_{rel},[d] kJ mol^{-1}
HBeBeH	**II**	−30.64502	15.672	283.9	0	−30.50519	394.2	306.0	0
BeH_2Be	**II***n*(3)	−30.57277	15.066	95.8	188.1	−30.45247	532.6	167.6	138.4
HBeMgH	**II**	−215.99828	12.796	211.2	0	−215.47632	356.1	238.6	0
BeHMgH	**II***n*(2)	−215.93582	9.645	55.5	155.7	−215.41900	506.6	107.4	131.2
HBeCaH	**II**	−693.47669	10.279	160.6	0	−692.85999	446.4	195.2	0
Be(H)CaH	**II***n*(2)	−693.44820	9.497	87.8	72.7	−692.83326	516.6	125.0	70.2
HMgMgH	**II**	−401.36254	10.299	166.3	0	−400.70952	302.2	198.1	0
MgHMgH	**II***n*(1)	−401.35777	9.518	155.8	10.5	−400.70317	318.9	181.4	16.7
$Mg(H)_2Mg$	**II***n*(3)	−401.34510	11.146	118.3	48.0	−400.69882	330.3	170.0	28.1
HMgCaH	**II**	−878.84695	8.426	129.8	0	−877.97125	376.5	165.1	0
HMgHCa	**II***n*(1)	−878.84103	9.808	110.6	19.2	−877.96717	387.2	154.4	10.7
Mg(H)CaH	**II***n*(2)	−878.84817	7.934	134.2	−4.5	−877.97122	376.6	165.0	0.1
$Mg(H)_2Ca$	**II***n*(3)	−878.84847	10.537	128.2	1.6	−877.97784	359.2	182.4	−17.3
HCaCaH	**II**	−1356.33489	7.473	100.0	0	−1355.23038	457.7	125.3	0
Ca(H)CaH	**II***n*(1)	−1356.34504	8.562	123.8	−23.8	−1355.24083	430.2	152.7	−27.4
$Ca(H)_2Ca$	**II***n*(3)	−1356.35195	10.203	137.7	−37.6	−1355.25512	392.7	190.2	−64.9

[a] Total energy, excluding ZPE.[b] [b] Zero-point vibrational energy. [c] Calculated bond dissociation energy, at the indicated level of theory (and at 0 K), for dissociation to HM + M′H. [d] Total energy, including ZPE, expressed relative to isomer **II**. [e] Total energy, including ZPE, at 0 K, according to G2(MP2)thaw calculations employing the B3-LYP/6-311+G** optimized geometry. [f] Calculated enthalpy of formation at 0 K.

nonclassical structures could be susceptible to experimental validation by a technique such as matrix isolation.

[MH_2M'] Structures. (These species contain two alkaline earth atoms; for consistency and clarity, we identify M′ as the heavier of the two group 2 atoms within the heterodinuclear compounds.) The classical structure HMM′H (**II**) is found to be linear for all M/M′ combinations except HMgCaH, for which an optimized structure with only very slight bending was obtained at the B3-LYP/6-311+G** level of theory, as detailed in Table 3. As with the group-1-containing [MHM′] species, the separation between the classical and nonclassical isomers is systematically much larger for compounds containing Be than is seen for compounds containing only Mg and/or Ca; the only structures possessing nonclassical global minima are [MgH_2-Ca] and [CaH_2Ca]. The [MgH_2Ca] potential energy surface is particularly rich, featuring three distinct nonclassical isomers in addition to the classical form. Our B3-LYP and G2(MP2) thaw calculations on the [MgH_2Ca] surface are in agreement regarding the slight difference in absolute energy between all four of these isomers (see Table 6) but disagree on assignment of the (apparently nonclassical) global minimum. Considering the spread of only about 30 kJ mol^{-1} over the energies of these species, a matrix-isolation study of these compounds might prove particularly interesting.

Of the general nonclassical structures, HMHM′ and MHM′H connectivities (**II***n*(1) and/or **II***n*(2)) were found to be local minima in several instances, as were doubly bridged structures MH_2M' (**II***n*(3)). These doubly bridged structures invariably also

TABLE 7: Calculated Total, Bond, and Relative Energies of Isomers on the [MH_3M'] PES

		B3-LYP/6-311+G**				G2(MP2)thaw			
formula	structure	E_e,[a] hartrees	ZPE,[b] mhartrees	D_0(M−M′),[c] kJ mol^{-1}	E_{rel},[d] kJ mol^{-1}	E_0,[e] hartrees	$\Delta H_f°$,[f] kJ mol^{-1}	D_0(M−M′),[c] kJ mol^{-1}	E_{rel},[d] kJ mol^{-1}
$HBeBH_2$	**XIII**	−41.34256	26.428	331.9	0	−41.18319	325.9	348.9	0
$HBe(H)_2B$	**XIII***n*(1)	−41.26211	24.025	126.9	204.9	−41.11137	514.5	160.4	188.6
$BeBH_3$	**XIII***n*(2)	−41.31236	27.101	250.8	81.1	−41.16153	382.8	292.1	56.8
$HBeAlH_2$	**XIII**	−258.95776	20.630	256.8	0	−258.41900	338.1	283.7	0
$HBe(H)_2Al$	**XIII***n*(1)	−258.97416	21.958	296.4	−39.6	−258.43274	302.0	319.8	−36.1
$BeAlH_3$	**XIII***n*(2)	−258.90821	19.424	129.9	126.9	−258.38012	440.1	181.7	102.0
$HBeGaH_2$	**XIII**	−1941.37774	20.627	263.6	0	−1939.88773	314.4	292.8	0
$HBe(H)_2Ga$	**XIII***n*(1)	−1941.40348	21.333	329.3	−65.7	−1939.90504	268.9	338.2	−45.4
$BeGaH_3$	**XIII***n*(2)	−1941.32147	19.712	118.2	145.3	−1939.84237	433.5	173.6	119.2
$HMgBH_2$	**XIII**	−226.68453	23.183	230.4	0	−226.14378	315.5	253.8	0
$HMg(H)_2B$	**XIII***n*(1)	−226.61741	20.584	61.0	169.4	−226.08251	476.4	92.9	160.9
$MgBH_3$	**XIII***n*(2)	−226.72784	27.364	333.2	−102.7	−226.18022	219.8	349.5	−95.7
$HMgAlH_2$	**XIII**	−444.31512	17.795	194.7	0	−443.39250	293.7	222.5	0
$HMg(H)_2Al$	**XIII***n*(1)	−444.31486	17.517	194.7	−0.1	−443.39432	288.9	227.3	−4.8
$MgAlH_3$	**XIII***n*(2)	−444.32902	19.255	227.4	−32.7	−443.40327	265.4	250.8	−28.3
$HMgGaH_2$	**XIII**	−2126.73553	17.749	202.7	0	−2124.98904	270.6	236.5	0
$HMg(H)_2Ga$	**XIII***n*(1)	−2126.74472	16.859	229.2	−26.5	−2124.99499	255.0	252.1	−15.6
$MgGaH_3$	**XIII***n*(2)	−2126.74257	19.502	216.6	−13.9	−2124.99578	252.9	254.2	−17.7
$HCaBH_2$	**XIII**	−704.16146	20.527	176.3	0	−703.52215	419.7	196.5	0
$HCaBH_2$	**XIII***r*	−704.16118	20.364	176.0	0.3	−703.52237	419.1	197.1	−0.6
$HCa(H)_2B$	**XIII***n*(1)	−704.12972	19.811	94.8	81.5	−703.49381	494.1	122.1	74.4
$CaBH_3$	**XIII***n*(2)	−704.21392	26.182	299.2	−122.9	−703.57506	280.8	335.4	−138.9
$HCaAlH_2$	**XIII**	−921.79765	15.252	155.0	0	−920.77768	380.1	183.1	0
$HCa(H)_2Al$	**XIII***n*(1)	−921.81133	14.746	192.2	−37.2	−920.79087	345.4	217.7	−34.6
$CaAlH_3$	**XIII***n*(2)	−921.81367	18.750	187.8	−32.9	−920.79533	333.7	229.4	−46.3
$HCaGaH_2$	**XIII**	−2604.21916	14.891	166.7	0	−2602.24855	350.8	197.7	0
$HCa(H)_2Ga$	**XIII***n*(1)	−2604.24075	14.109	225.4	−58.7	−2602.26378	310.8	237.7	−40.0
$CaGaH_3$	**XIII***n*(2)	−2604.22823	18.909	180.0	−13.3	−2602.25870	324.1	224.3	−26.6

[a] Total energy, excluding ZPE.[b] [b] Zero-point vibrational energy. [c] Calculated bond dissociation energy, at the indicated level of theory (and at 0 K), for dissociation to HM + M′H_2. [d] Total energy, including ZPE, expressed relative to isomer **XIII**. [e] Total energy, including ZPE, at 0 K, according to G2(MP2)thaw calculations employing the B3-LYP/6-311+G** optimized geometry. [f] Calculated enthalpy of formation at 0 K.

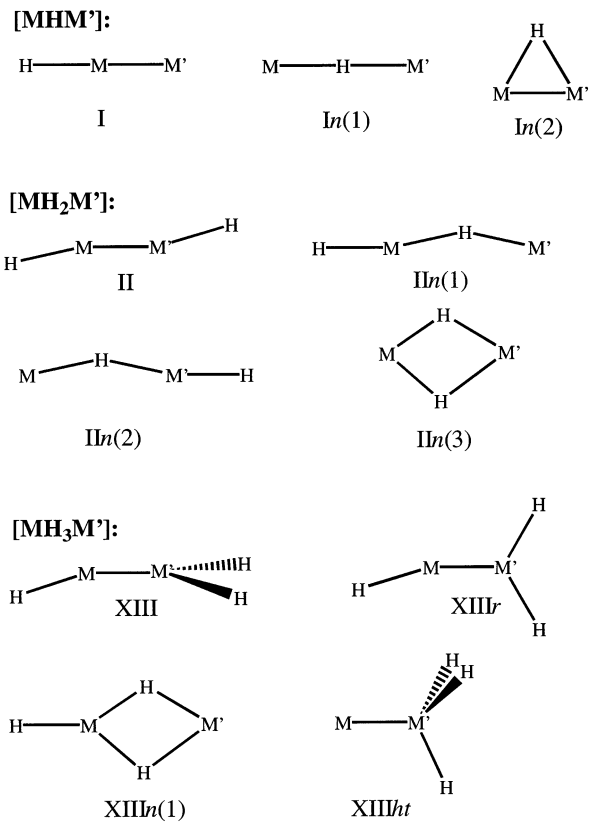

Figure 1. General scheme of structural motifs encountered among the [MHM′], [MH_2M′], and [MH_3M′] stationary points at the B3-LYP/6-311+G** level of theory.

featured M−M′ separations characteristic of intermetallic bond formation (see Table 3), but these short M−M′ bonds were present in only half the singly bridged structures (M−M′ bonds were present in the MHCaH structures but not in HBeHMg, HMgHMg, or HMgHCa). No minima were found for BeHM′H configurations, nor for $Be(H)_2$M′ doubly bridged structures with the exception of $Be(H)_2Be$ (which is seen to be thermodynamically unstable to dissociation to Be + HBeH according to the bond energies in Table 8. We have, however, confirmed that BeH_2Be has reasonable *kinetic* stability, according to G2(MP2)-thaw calculations, which indicate that the open-shell singlet transition state to Be atom loss has a total energy 38.1 kJ mol^{-1} greater than that of the BeH_2Be local minimum). The existence of a direct M−M′ bond in doubly bridged structures **II***n*(3) is perhaps a structural necessity: if each M is bonded to both H atoms, it is probably not possible to separate the two atoms sufficiently far to cleave the M−M′ bond without also destroying at least one of the hydrogen bridges. However, metal−metal bonding is clearly not so geometrically preordained for the **II***n*(1) and **II***n*(2) isomers: the presence of a M−M′ bond in the MHCaH structures, and the absence of such bonding in the other examples, is consistent with the much greater accessibility of vacant (3*d*) orbitals on the calcium atom than for Be or Mg. It is also notable that the BeHMgH and MgHMgH minima feature very long M···MgH separations, indicating that these species are best considered as van der Waals "dimers" of M with HMgH. Their bond strengths against this mode of dissociation are listed in Table 8 where the data for HMgH···Ca are seen to be strikingly different, possibly because of the facility of Ca for forming long bonds using *d* orbitals.

Some comparison with experiment is possible for the systems [BeH_2Be] and [MgH_2Mg], both of which have been studied by matrix isolation of reaction products from laser-ablated alkaline-earth atoms with H_2 in an argon buffer gas.[3,4] In the former case, only the classical structure HBeBeH **II** was observed, on the basis of IR spectroscopy undertaken in conjunction with ab

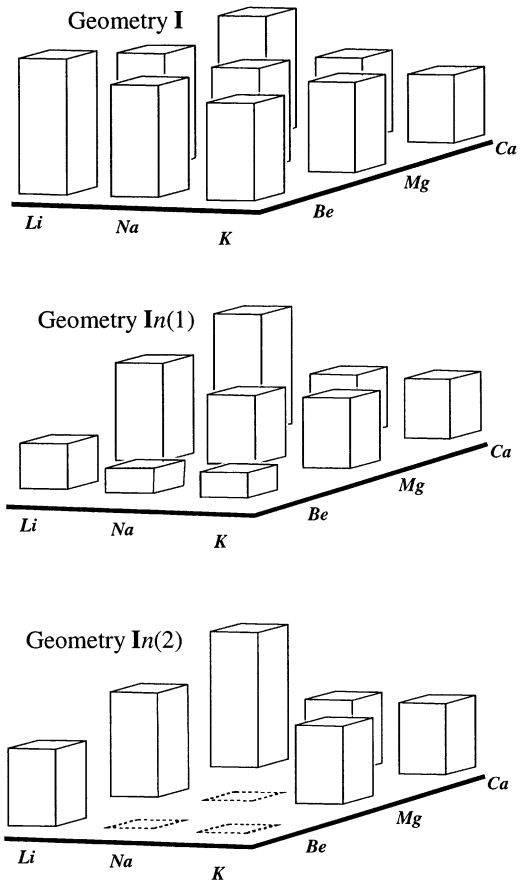

Figure 2. Schematic representation of bond strength trends for the various structural motifs encountered on the [MHM′] potential energy surface. Column height corresponds to the M−M′ bond dissociation energy as obtained from our G2MP2(thaw) calculations. Dashed outlines indicate a stationary point that is not stable for a given combination of M and M′.

initio (MP2/6-31G*) calculation of spectroscopic and energetic parameters for the various isomers.[3] The calculations of Tague and Andrews placed all possible nonclassical structures at much higher energies than the global minimum **II**, with relative energies from their calculations (E_{rel}(**II***n*(3)) = 192 kJ mol^{-1})[3] showing good agreement with our B3-LYP calculations but significantly overestimating the energy difference obtained from our G2(MP2)thaw calculations (E_{rel}(**II***n*(3)) = 138 kJ mol^{-1}). The relative energies of **II** and **II***n*(3) have also been addressed in calculations performed by Bruna et al.,[16] who report E_{rel}-(**II***n*(3)) ∼ 164 kJ mol^{-1} on the basis of SCF calculations.

The matrix-isolation investigation of [MgH_2Mg],[4] employing also MP2/6-31G* calculations in support of laboratory spectroscopic data, reported the experimental detection of two [MgH_2Mg] isomers, **II** and **II***n*(3), with nonclassical **II***n*(3) being the higher-energy isomer (E_{rel}(**II***n*(3)) = 53 kJ mol-^{1});[4] again, agreement of this MP2/6-31G* value with our B3-LYP value is good but our G2(MP2)thaw calculations show the gap between **II** and **II***n*(3) to be significantly less than this. A more notable disagreement between their calculations and ours concerns the third isomer, MgHMgH (**II***n*(1)), which was not apparently detected in their matrix-isolation experiment and for which they obtained E_{rel}(**II***n*(1)) = 176 kJ mol^{-1} at the MP2/6-31G* level of theory;[4] their calculations show this isomer to be unstable with respect to the separated products MgH + MgH (E_{rel} = 170 kJ mol^{-1}) and Mg + HMgH (E_{rel} = 18 kJ mol^{-1}), where E_{rel} indicates the calculated total energy of the identified product combination relative to that of classical HMgMgH. In contrast, our B3-LYP and G2(MP2)thaw calculations place MgHMgH (**II***n*(1)) only 10−20 kJ mol^{-1} above the global minimum **II**. The absence of MgHMgH from the products identified by Tague and Andrews in their matrix-isolation study[4] can, nevertheless, be easily rationalized in view of the extremely low strength of the Mg···MgH bond, as detailed in Table 8.

[CaH_2Ca] has also been featured in a FT/IR matrix isolation study,[5] which reported identification of the classical structure **II** but did not detect either of the nonclassical isomers **II***n*(1) or **II***n*(3), which we calculate to be the two lowest-energy structures.

TABLE 8: Calculated M−M′H$_{j+1}$ Bond Strengths for Relevant Nonclassical Minima, Obtained at the G2(MP2)Thaw Level of Theory

formula	structure	D_0(M−M′H$_{j+1}$), kJ mol^{-1}
	[MHM′]	
BeHLi	**I***n*(1)	15.2
Be(H)Li	**I***n*(2)	55.1
MgHLi	**I***n*(1)	15.9
Mg(H)Li	**I***n*(2)	25.0
CaHLi	**I***n*(1)	72.4
Ca(H)Li	**I***n*(2)	92.4
BeHNa	**I***n*(1)	35.1
MgHNa	**I***n*(1)	21.6
CaHNa	**I***n*(1)	38.2
Ca(H)Na	**I***n*(2)	49.4
BeHK	**I***n*(1)	54.1
MgHK	**I***n*(1)	39.3
Mg(H)K	**I***n*(2)	48.8
CaHK	**I***n*(1)	55.6
Ca(H)K	**I***n*(2)	66.6
	[MH_2M']	
BeH_2Be	**II***n*(3)	−34.2
BeHMgH	**II***n*(2)	0.9
Be(H)CaH	**II***n*(2)	63.8
MgHMgH	**II***n*(1)	1.7
$Mg(H)_2Mg$	**II***n*(3)	−9.7
HMgHCa	**II***n*(1)	19.7
Mg(H)CaH	**II***n*(2)	30.3
$Mg(H)_2Ca$	**II***n*(3)	32.0[a]
Ca(H)CaH	**II***n*(1)	47.3
$Ca(H)_2Ca$	**II***n*(3)	84.8
	[MH_3M']	
$BeBH_3$	**XIII***ht*	40.0
$BeAlH_3$	**XIII***ht*	16.2
$BeGaH_3$	**XIII***ht*	20.2
$MgBH_3$	**XIII***ht*	29.5
$MgAlH_3$	**XIII***ht*	17.4
$MgGaH_3$	**XIII***ht*	27.3
$CaBH_3$	**XIII***ht*	39.1
$CaAlH_3$	**XIII***ht*	19.7
$CaGaH_3$	**XIII***ht*	26.6

[a] The value shown is $D_0(Mg(H)_2-Ca)$. For the alternative mode of dissociation, $D_0(Mg-(H)_2Ca)$ = 47.7 kJ mol^{-1}.

[MH_3M'] Structures. One noteworthy result for these group-13-containing species is that [BeH_3B] is the only instance for which the orthodox structure **XIII** is the global minimum. For [BeH_3Al], [BeH_3Ga] and [CaH_3Ga], the lowest-energy structure is **XIII***n*(1); for [MgH_3B], [MgH_3Al] and [CaH_3B] the global minimum is the classical but unorthodox species **XIII***ht*, whereas for each of [MgH_3Ga] and [CaH_3Al] our calculations show two low-lying unorthodox possibilities but do not reliably identify the lower of the two.

This class of compounds, for M = Be, Mg, and Ca and M′ = B and Al, have been the subject of a previous series of investigations by Charkin and co-workers.[19,20,22,23] These earlier studies employed the 6-31G* basis set and treatment of electron correlation up to MP4 but did not include vibrational frequency

calculations that are critical to the identification of stationary points as either minima or *n*-order saddle points. Consequently, although competition between orthodox forms **XIII** and unorthodox structures is a motif in their studies, as in ours, there are considerable discrepancies evident between their work[19,20,22,23] and ours regarding the identity of the unorthodox minima. In their study on [MH_3B] structures,[19] they do not report any investigation of **XIII***n*(1) or **XIII***ht*, which we consistently find to be minima at the B3-LYP/6-311+G** level of theory, instead exploring structures with the connectivities $MHBH_2$ and $M(H)_2$-BH, which we shall refer to as **XIII***n*(3) and **XIII***n*(4), respectively. Neither **XIII***n*(3) nor **XIII***n*(4) is a minimum at the B3-LYP/6-311+G** level of theory: this holds, also, for M′ = Al and Ga. The [MH_3Al] calculations of Charkin and co-workers[20,22,23] do not consider **XIII***ht*, **XIII***n*(3), or **XIII***n*(4) but do include a species H_2MHAl, **XIII***n*(5), which we find to be a first- or second-order saddle point in all cases (true also for M′ = B and Ga). At the MP3/6-31G* level,[20,22,23] calculations of the relative energies of **XIII** and **XIII***n*(1) are in reasonable agreement with our results for [MH_3Al]. Our results are in agreement, also, with the general finding by Charkin and co-workers[20,22,23] that the Al-containing species all feature unorthodox global minima.

The identification of **XIII***ht* as a local (and, in several cases, global) minimum is of considerable interest, not least because such species should be very readily susceptible to formation and rare-gas matrix isolation by straightforward combination of the laser-ablated alkaline earth atom M with $M'H_3$. An analysis of the relative energies of isomers in Table 7, and of the M−M′H_3 bond strengths detailed in Table 8, suggests that $MgBH_3$ and $CaBH_3$ would be particularly promising candidates for such isolation.

What factors influence the stability of such structures as **XIII***ht*? Clearly, although the absolute M−M′H_3 bond strengths are universally rather low (see Table 8), this is in many cases offset by the formation of a third M′−H bond of characteristically greater strength than the H−M bond that is lost, so that for several examples **XIII***ht* is the global minimum as noted above. The nominally tetrahedral coordination around M′ suggests a promotion from sp^2 to sp^3 hybridization around this atom; the low M−M′ bond strengths, and the minor increase in the MM′H bond angle (from 90° to a maximum value of 95.0°, seen for the example of $BeBH_3$), both serve to indicate only a modest increase in the p character of the M′−H bonds.

Rationalizing the Polyisomerism: An Atoms-in−Molecules Analysis. The metals of the block comprising the first three main-group columns of the periodic table have very low electronegativities (all lower than hydrogen) and their solid hydrides are predominantly saltlike (metal cations, hydride anions). Covalence starts to matter for metals close to the top and the right of the block and the bonds can be very strong (the B−H bond in BH_3 is as strong as the H_2 bond). Despite this, these elements are famous for their ability to compensate for a deficiency of electrons by forming multicenter bonds. These features clearly must enter the explanation for the unexpectedly numerous hydrogen-bridged structures that compete with classical hydrides for a place on the potential energy surfaces. The discussion that follows relates particularly to the alkali-metal-containing [MHM′] series of compounds.

Bond type is not easy to characterize, especially in such compounds as the hydrides studied here. One approach used here is atoms-in-molecules (AIM) analysis[27] of the electron density. Knowing whether the electron density has been depleted or concentrated between atoms that are close together may allow us to classify the interactions as closed-shell type or covalent type, signaled by the sign of the Laplacian of the electron density at the bond critical point [$\nabla^2\rho(r_c)$].[27] The simple hydrides of the nine metals (Li, Na, K; Be, Mg, Ca; B, Al, Ga) all yield electron density distributions with positive $\nabla^2\rho(r_c)$, the usual indicator of a closed shell interaction. However, for some of these the density itself at the bond critical point [$\rho(r_c)$] is higher than it typically is for electrostatically bound compounds and must be due to charge concentration in the space between the atoms resulting from electron sharing; they thus seem to be intermediate between a closed-shell and a shared (covalent) interaction. We judge BeH_2, BH_3, AlH_3, and GaH_3 to fall into the "intermediate" category. For the data, see Table 9.

TABLE 9: AIM Bond Orders and Other Properties of the Electron Density of Simple Hydrides Calculated at the B3-LYP/6-311+G Level of Theory**

AH_n	$D_0(AH_{n-1}-H)$ kJ mol^{-1}	χ–(Pauling)[a]	$\nabla^2\rho(r_c)$[b]	$\rho(r_c)$[c]	ρ_{AH}[d]	formal charge[e] q_A	formal charge[e] q_H
LiH	235	0.98	0.163	0.040	0.228	0.895	−0.895
NaH	181	0.93	0.131	0.033	0.535	0.716	−0.715
KH	168	0.82	0.076	0.030	0.525	0.741	−0.741
BeH_2	386	1.57	0.143	0.099	0.331	1.654	−0.828
MgH_2	285	1.31	0.218	0.053	0.475	1.502	−0.752
CaH_2	242	1.00	0.109	0.047	0.460	1.567	−0.783
BH_3	430	2.04	0.343	0.184	0.630	1.831	−0.611
AlH_3	340	1.61	0.262	0.081	0.485	2.210	−0.737
GaH_3	326	1.81	0.101	0.116	0.899	1.228	−0.410
H_2	434	2.10	−0.106	0.261	1.000	0.000	0.000

[a] Pauling electronegativity of the atom A. [b] Laplacian of the electron density at the A−H bond critical point r_c. [c] Electron density at the A−H bond critical point r_c. [d] AIM bond order ρ_{AH} for the A−H bond. [e] AIM formal charge on the specified atom within AH_n.

TABLE 10: Calculated AIM Data for Individual Bonds Obtained at the B3-LYP/6-311+G Level of Theory**

bond	structure	$\nabla^2\rho(r_c)$[a]	$\rho(r_c)$[b]	bond order[c]	formal charge[d] q_H	formal charge[d] q_{Na}	formal charge[d] q_{Ca}
Na−H		0.131	0.033	0.535	−0.715	0.715	−
HCa−H		0.109	0.047	0.460	−0.783	−	1.567
H−CaNa	**I**	0.109	0.050	0.493	−0.767	−0.167	0.600
HCa−Na	**I**	−0.001	0.011	0.960	−0.767	−0.167	0.600
CaH−Na	**I***n*(1)	0.101	0.026	0.339	−0.776	0.565	0.211
Ca−HNa	**I***n*(1)	0.071	0.028	0.366	−0.776	0.565	0.211
Ca(H)-Na	**I***n*(2)	0.090	0.023	0.190	−0.817	0.610	0.207
Ca−(H)Na	**I***n*(2)	0.082	0.043	0.473	−0.817	0.610	0.207

[a] Laplacian of the electron density at the A−H bond critical point r_c. [b] Electron density at the bond critical point r_c for the specified bond. [c] AIM bond order for the specified bond. [d] AIM formal charge on the specified atom.

The calculated metal−metal bond lengths of the [MHM′] series compounds permit one additional comment on bond type. Among the classical (type **I**) structures, the bond lengths range from 0 to 8% shorter than the sums of the covalent radii, which are generally at least 50% larger than the sums of the ionic radii. So, clearly, the bond-forming behavior of these metals is that of elements forced into electron sharing, however long and weak the resulting bonds may be.

To shed further light on the bonding within all three structural types accessible to [MHM′], we have analyzed the compound [CaHNa] in the three isomeric forms **I**, **I***n*(1) and **I***n*(2) in which it appears at true minima on the PE surface (see Table 10). The AIM results suggest that (a) whenever Ca or Na are adjacent to a hydrogen they are attached to it electrostatically, (b) that the Ca−Na bond in the I structure is covalent but very weak and (c) that the triangular **I***n*(2) structure is in the curious position of having a fairly large shared density between the Ca and Na

atoms without there being any bond (no interatomic surface or bond critical point). In other words, the bonds in the **I***n*(1) isomer remain in almost the same form when it bends to produce the **I***n*(2) form.

A small computational experiment was performed on the [CaHNa] isomers, in which the effective nuclear charge parameters governing the one-electron wave functions of the Ca and Na atoms were slightly changed in one direction and then the other. The result was the same for all three structure types: When Na was artificially made more electronegative, the energy [D_0(M−M′)] required to form HCa$^\bullet$ and Na$^\bullet$ always increased and the Ca−Na bond length always increased. When Ca was made more electronegative, the energy was always slightly lessened and the Ca−Na bond length decreased. These results, if generalizable, explain why the compounds of the least electronegative element Li are usually the most stable of the three alkali metal compounds in each category but it is hard to use them to rationalize the complex relationships between the Be, Mg, and Ca series in the three structure types.

The results of population analysis yield some useful comparisons between the three isomers found for [CaHNa] and the other [MHM′] compounds. For all three structure types the evidence suggests that electrostatic binding is important but that it is supplemented by covalence, without which the classical HMM′ isomers could not exist. The formal charges calculated under the AIM procedure are 0.17 for sodium (not 1.0) and 0.60 for calcium (not 2.0), implying considerable sharing and rearrangement of electronic charge.

The electron sharing displayed by the classical HMM′ isomers is at the level expected for s-block metals with Pauling electronegativities ranging from 0.82 (K) to 1.57 (Be), all substantially lower than the value for H (2.1). The Ca−Na bond is long and fairly weak and it has the unusual combination of a very small but negative value of the Laplacian at the bond critical point and a large AIM bond order. With both cations on the same side of the H^- ion the disposition of electronic charge between Ca and Na favors electron sharing and produces a D_0(M−M′) value of 85.6 kJ mol^{-1}.

In the linear nonclassical isomer Ca−H−Na [the **I***n*(1) structure] the presence of a cation on each side of the hydride ion reverses the flows of electronic charge from the two metal atoms and yields smaller AIM bond orders together with the positive values of the Laplacian expected for closed shell interactions between two cations and a hydride ion.

The triangular arrangement is interesting. In every one of the nine possible cases, bending the linear **I***n*(1) structure at the H atom through an angle of about 90° produces a structure that requires 50 kJ mol^{-1} or more of energy to disrupt, [D_0(M−M′)] but in three of the nine cases the structure lies on a slope of the energy surface at this configuration and, for these three cases, no stable **I***n*(2) isomer exists as it does for the compound [CaHNa] and the other five compounds. The stability of the bent isomers cannot be attributed to any angular preference at the hydrogen atom (the population of p-type polarization functions in the molecular wave function is minute) so it must be due to some characteristic of the charge cloud induced around hydrogen by two cations that allows enhanced bonding even at the expense of the repulsion that necessarily appears between the two approaching cations. All six species for which **I***n*(2) is a local minimum display a MHM′ angle of about 90°.

The stability conferred on the compound by bending at hydrogen to produce **I***n*(2) isomers, though not large, is notable for the following reasons. The interaction between metal atoms in **I***n*(2) isomers is repulsive because electron transfer to hydrogen leaves them both with a net positive charge. AIM analysis reveals no critical point on any path between the two atoms so there is no favorable contribution to the bending process. This, together with the energy data for **I***n*(2) isomers leads to the conclusion that the intrinsic strength of the M−H and M′−H bonds in the bent configuration is greater than that of the bonds holding the **I** and **I***n*(1) isomers together because it has to overcome the M−M′ repulsion. This repulsion must be quite large, because in every case in which an **I***n*(2) isomer exists, the M−M′ separation is smaller than in the classical isomer. (The distance between Na and Ca is 316.4 pm in the **I***n*(2) isomer and 342.9 pm in the classical isomer.) This puzzling aspect of the intermetallic interaction, which may very well apply in all of the [$MH_{j+1}M'$] compounds featuring a markedly noncollinear M(H)M′ functionality, clearly warrants further investigation.

General Discussion. It is notable that, of the species explored in the present study, only the "homonuclear dimers" [BeH_2-Be], [MgH_2Mg], and [CaH_2Ca] have yet been subjected to experimental investigation,[3−5] whereas previous theoretical studies have dealt almost exclusively with the hydrides [$MH_{j+1}M'$] formed by combination of first-and second-row M and M′. The lack of any previous laboratory study on "mixed-metal" hydrides reflects the greater experimental difficulties in distinguishing between a number of weakly stable structures when the "melting pot" comprises three different elements, rather than merely two; similarly, the paucity of computational efforts on third-row-containing hydrides (most notably, the complete absence of any previous studies on [MHK] or [MH_3Ga] species) is also indicative of the greater requirement for computational resources on higher-atomic-number atoms. Our own calculations on these somewhat more troublesome species indicate that they do, indeed, merit further study, by virtue of the novel bonding configurations they adopt, and the scope they offer for a more detailed understanding of covalent interactions between electron-poor atoms.

Conclusions

Our calculations on alkaline-earth-containing dinuclear metal hydrides have revealed several notable examples of nonclassical structures among such compounds, with some of these nonclassical structures (most particularly, among the group-13-element-containing [MH_3M'] species) identifiable as the global minima on their respective potential energy surfaces. A consistent feature of these potential energy surfaces is the competition between "classical covalent" dinuclear species of the generic formula $HMM'H_{j-1}$ and nonclassical (or otherwise unorthodox) complexes of an alkaline earth atom with the monomeric hydride $M'H_j$. The strength of such nonclassical interactions can vary widely, with the Be···HMgH and Mg···HMgH complexes so fragile that their experimental isolation appears extremely unlikely; in contrast, M···$M'H_n$ bond strengths approaching 100 kJ mol^{-1} are found for Ca with LiH and CaH_2, suggesting that these are particularly good candidates for laboratory study. We have also identified the symmetric tops M−$M'H_3$, particularly with M′ = B, as another set of compounds that possess an unusual bonding configuration and that may be of further interest to experimentalists.

AIM (atoms-in−molecules) calculations undertaken on some representative structures among those surveyed here reveal that the intermetallic interaction is essentially covalent in character. Nevertheless, the molecular motivation behind several of the geometric preferences exhibited by this class of compounds remains mysterious.

Acknowledgment. We thank the Australian Research Council for financial support of this research.

References and Notes

(1) Leszczynski, J.; Lammertsma, K. *J. Phys. Chem.* **1991**, *95*, 3941.

(2) In unpublished B3-LYP/6-311+G** calculations undertaken in the course of our survey of main-group single bonds, we have located a ninth isomer of [AlH_4Ga], which can be described as $HAl(H)GaH_2$, and which is confirmed as a (comparatively high-lying) local minimum according to vibrational frequency calculations.

(3) Tague, T. J., Jr.; Andrews, L. *J. Am. Chem. Soc.* **1993**, *115*, 12111.

(4) Tague, T. J., Jr.; Andrews, L. *J. Phys. Chem.* **1994**, *98*, 8611.

(5) Xiao, Z. L.; Hauge, R. H.; Margrave, J. L. *High Temp. Sci.* **1991**, *31*, 59.

(6) Hodošcek, M.; Šolmayer, T. *J. Am. Chem. Soc.* **1984**, *106*, 1854.

(7) Kaufmann, E.; Tidor, B.; Schleyer, P. v. R. *J. Comput. Chem.* **1986**, *7*, 334.

(8) Sannigrahi, A. B.; Kar, T. *J. Mol. Struct. (THEOCHEM)* **1988**, *180*, 149.

(9) Tikilyainen, A. A.; Zyubin, A. S.; Charkin, O. P. *Russ. J. Inorg. Chem.* **1989**, *34*, 613.

(10) Sana, M.; Leroy, G. *Theor. Chim. Acta* **1990**, *77*, 383.

(11) Anders, E.; Koch, R.; Freunscht, P. *J. Comput. Chem.* **1993**, *14*, 1301.

(12) Kar, T.; Jug, K. *J. Mol. Struct. (THEOCHEM)* **1993**, *283*, 177.

(13) Graham, G. D.; Marynick, D. S.; Lipscomb, W. N. *J. Am. Chem. Soc.* **1980**, *102*, 4572.

(14) Jasien, P. G.; Dykstra, C. E. *J. Am. Chem. Soc.* **1985**, *107*, 1891.

(15) Mebel, A. M.; Klimenko, N. M.; Charkin, O. P. *Russ. J. Inorg. Chem.* **1991**, *36*, 419.

(16) Bruna, P. J.; Di Labio, G. A.; Wright, J. S. *J. Phys. Chem.* **1992**, *96*, 6269.

(17) Lauvergnat, D.; Hiberty, P. C. *J. Mol. Struct. (THEOCHEM)* **1995**, *338*, 283.

(18) Hashimoto, K.; Osamura, Y.; Iwata, S. *J. Mol. Struct. (THEOCHEM)* **1987**, *152*, 101.

(19) Bonaccorsi, R.; Charkin, O. P.; Tomasi, J. *Inorg. Chem.* **1991**, *30*, 2964.

(20) Zyubin, A. S.; Gorbik, A. A.; Charkin, O. P. *Zh. Strukt. Khim.* **1988**, *29*, 502.

(21) Jasien, P. G.; Dykstra, C. E. *J. Am. Chem. Soc.* **1983**, *105*, 2089.

(22) Zyubin, A. S.; Gorbik, A. A.; Charkin, O. P. *Zh. Strukt. Khim.* **1988**, *29*, 9.

(23) Zyubin, A. S.; Charkin, O. P. *Zh. Strukt. Khim.* **1990**, *31*, 373.

(24) Leroy, G.; Sana, M.; Wilante, C.; van Zieleghem, M.-J. *J. Mol. Struct.* **1991**, *247*, 199.

(25) Sana, M.; Nguyen, M. T. *Chem. Phys. Lett.* **1992**, *196*, 390.

(26) Ochterski, J. W.; Petersson, G. A.; Wiberg, K. B. *J. Am. Chem. Soc.* **1995**, *117*, 11299.

(27) Bader, R. F. W. *Atoms in Molecules: A Quantum Theory*; Oxford University Press: Oxford, U.K., 1990.

(28) Curtiss, L. A.; Raghavachari, K.; Trucks, G. W.; Pople, J. A. *J. Chem. Phys.* **1991**, *94*, 7221.

(29) Curtiss, L. A.; Raghavachari, K.; Pople, J. A. *J. Chem. Phys.* **1993**, *98*, 1293.

(30) Curtiss, L. A.; McGrath, M. P.; Blaudeau, J.-P.; Davis, N. E.; Binning, R. C., Jr.; Radom, L. *J. Chem. Phys.* **1995**, *103*, 6104.

(31) Blaudeau, J.-P.; McGrath, M. P.; Curtiss, L. A.; Radom, L. *J. Chem. Phys.* **1997**, *107*, 5016.

(32) Duke, B. J.; Radom, L. *J. Chem. Phys.* **1998**, *109*, 3352.

(33) Petrie, S. *Chem. Phys. Lett.* **1998**, *283*, 181.

(34) Petrie, S. *J. Phys. Chem. A* **1998**, *102*, 6138.

(35) Schulz, A.; Smith, B. J.; Radom, L. *J. Phys. Chem. A* **1999**, *103*, 7522.

(36) Bauschlicher, C. W., Jr.; Melius, C. F.; Allendorf, M. D. *J. Chem. Phys.* **1999**, *110*, 1879.

(37) Frisch, M. J.; Trucks, G. W.; Schegel, H. B.; Scuseria, G. E.; Robb, M. A.; Cheeseman, J. R.; Zakrzewski, V. G.; Montgomery, J. A., Jr.; Stratmann, R. E.; Burant, J. C.; Dapprich, S.; Millam, J. M.; Daniels, A. D.; Kudin, K. N.; Strain, M. C.; Farkas, O.; Tomasi, J.; Barone, V.; Cossi, M.; Cammi, R.; Mennucci, B.; Pomelli, C.; Adamo, C.; Clifford, S.; Ochterski, J. W.; Petersson, G. A.; Ayala, P. Y.; Cui, Q.; Morokuma, K.; Malick, D. K.; Rabuck, A. D.; Raghavachari, K.; Foresman, J. B.; Cioslowski, J.; Ortiz, J. V.; Stefanov, B. B.; Liu, G.; Liashenko, A.; Piskorz, P.; Komaromi, I.; Gomperts, R.; Martin, R. L.; Fox, D. J.; Keith, T.; Al-Laham, M. A.; Peng, C. Y.; Nanayakkara, A.; Gonzalez, C.; Challacombe, M.; Gill, P. M. W.; Johnson, B. G.; Chen, W.; Wong, M. W.; Andres, J. L.; Head-Gordon, M.; Replogle, E. S.; Pople, J. A. *Gaussian98*; Gaussian, Inc.: Pittsburgh, PA, 1998.